Controlling the dispersion of Co_3O_4 nanoparticles inside mesoporous nanorattle catalysts

Zacho, Simone Louise; Hyllested, Jes Æ.; Kasama, Takeshi; Mielby, Jerrik Jørgen

Published in:
Catalysis Communications

Link to article, DOI:
10.1016/j.catcom.2019.02.020

Publication date:
2019

Document Version
Peer reviewed version

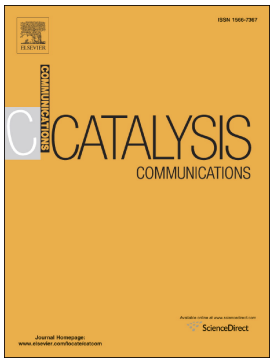

Controlling the dispersion of Co_3O_4 nanoparticles inside mesoporous nanorattle catalysts

Simone L. Zacho, Jes.Æ. Hyllested, Takeshi Kasama, Jerrik Mielby

PII: S1566-7367(19)30054-8
DOI: https://doi.org/10.1016/j.catcom.2019.02.020
Reference: CATCOM 5631

To appear in: *Catalysis Communications*

Received date: 15 November 2018
Revised date: 31 January 2019
Accepted date: 21 February 2019

Please cite this article as: S.L. Zacho, J.Æ. Hyllested, T. Kasama, et al., Controlling the dispersion of Co_3O_4 nanoparticles inside mesoporous nanorattle catalysts, Catalysis Communications, https://doi.org/10.1016/j.catcom.2019.02.020

Controlling the Dispersion of Co_3O_4 Nanoparticles inside Mesoporous Nanorattle Catalysts

Simone L. Zacho,[a] Jes. Æ. Hyllested,[b] Takeshi Kasama[b] and Jerrik Mielby[a,*] jjmie@kemi.dtu.dk

[a]DTU Chemistry, Technical University of Denmark, Kemitorvet 207, 2800 Kgs. Lyngby, Denmark
[b]DTU Center for Electron Nanoscopy, Technical University of Denmark, Fysikvej 307, 2800 Kgs. Lyngby, Denmark

[*]Corresponding author.

Abstract

Here we report a simple method to synthesize cobalt nanoparticles inside mesoporous nanorattle catalysts. In this method, zeolitic imidazolate framework ZIF-67 is used as structural template for the preparation of a mesoporous metal oxide shell as well as sacrificial precursor to form cobalt nanoparticles inside the shell. Furthermore, we demonstrate that the introduction of a carbonization step prior to the final calcination can decrease the required calcination temperature from 550 °C to 300 °C. This has a large effect on the dispersion and catalytic activity of Co_3O_4 for CO oxidation and decreases the light-of temperature (temperature at 50% conversion) from 160°C to 134°C. Exploiting metal-organic frameworks as both structural template and sacrificial precursor offers precise control of size, shape and structure and opens up new exiting opportunities for design of advanced nanostructured catalysts.

Keywords: metal-organic frameworks, mesoporous materials, templating, nanorattle catalysts, CO oxidation

1. Introduction

The rational design and synthesis of hollow nanostructured materials holds great promise for new and emerging technologies in fields ranging from energy storage,[1–3] catalysis,[4] adsorption,[5] separation,[6] sensing,[7] photocatalysis[8] to drug delivery.[9,10] Besides their high porosity, high surface area and low density, the hollow nanomaterials offer a number of key advantages with respect to loading or functionalization of their interior.[11] Furthermore, hollow nanostructures may help to prevent aggregation, sintering and metal leaching.[12] In particular, these advantages have been intensely pursued in confined synthesis,[13] nanoreactors[4,14] and controlled release.[15]

There are several methods to prepare hollow nanomaterials. These methods are typically based on 'templating' using either hard[16] or soft templates[17–19]. Alternative template-free methods based on the Kirkendall effect,[20] Ostwald ripening,[21] selective dissolution[22] or recrystallization are also available.[23] All these methods have different advantages and disadvantages, but typically suffer from complicated synthesis procedures, expensive additives, poor yield or non-uniform materials. Subsequent loading or functionalization often causes further challenges and limitations. This has encouraged researchers to continue finding new and effective methods to synthesize hollow nanomaterials in simple and economically viable ways.

Metal-organic frameworks (MOFs) consist of metal ions or clusters that are coordinated by organic linkers to form three-dimensional structures. The tunable porosity of these structures gives rise to remarkable physical properties with many promising applications in gas storage, separation and catalysis.[24,25]

Furthermore, MOFs have recently attracted much interest as sacrificial precursors for preparation of porous N-doped carbons for applications in electrochemistry.[26,27] Here we demonstrate how a type of MOFs known as zeolitic imidazolate frameworks (ZIFs) represents a promising platform for the design and synthesis of heterogeneous nanorattle catalysts. Furthermore, we show how the carbonization and/or calcination of the ZIFs controls the three-dimensional distributions of metal nanoparticles inside the nanorattles.

In the first step, ZIF-67 is synthesized from a solution of cobalt(II) nitrate and 2-methyl imidazole in methanol. We then exploit the ZIF-67 as structural template for the synthesis of a shell of mesoporous silica using tetra ethyl orthosilicate (TEOS) and cetyltrimethylammonium bromide (CTAB). The composite material is then calcined in order to decompose the ZIF-67 core into Co_3O_4 and remove the organic template by combustion. This process requires a temperature of >550 °C. However, if the material is first carbonized under inert atmosphere, the ZIF-67 is decomposed into small Co nanoparticles stabilized by a N-doped carbon matrix inside the shell. Although this carbonization step is performed at 600 °C, the subsequent calcination to remove the N-doped carbon and oxidize Co into Co_3O_4 already occur at 300 °C, see **Error! Reference source not found.**. Sequential carbonization and calcination therefore results in less sintered and smaller cobalt oxide nanoparticles than possible by direct calcination of ZIF-67. Table 1 shows a schematic outline of the synthetic procedure and the prepared materials.

Table 1. Outline of the synthetic procedure and the prepared materials.

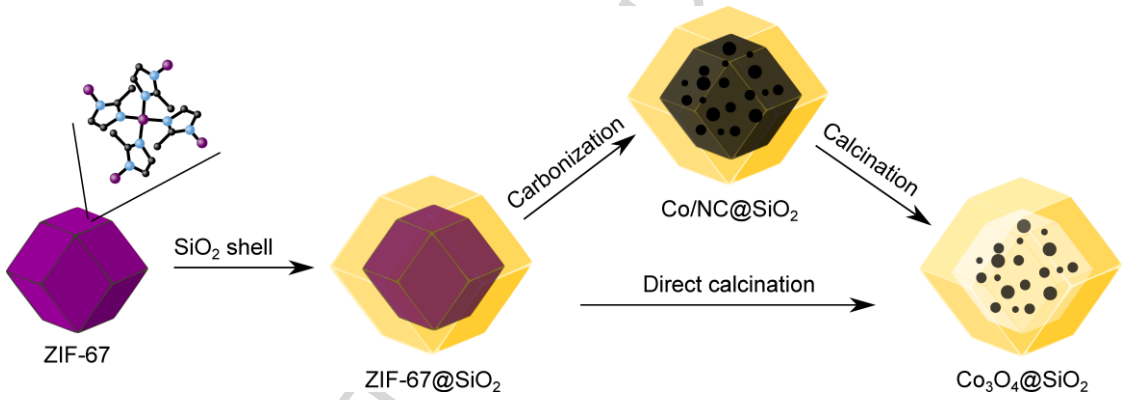

Entry	Material	Carbonization temp.	Calcination temp.
1	ZIF-67@SiO_2	-	-
2	Co_3O_4@SiO_2 (-/550)	-	550 °C
3	Co/NC@SiO_2 (600/-)	600 °C	-
4	Co_3O_4@SiO_2 (600/550)	600 °C	550 °C
5	Co_3O_4@SiO_2 (600/300)	600 °C	300 °C

2. Results and discussion

The ZIF-67@SiO_2 core-shell material was characterized by X-ray powder diffraction (XRD) to verify the successful synthesis of ZIF-67. The XRD pattern showed the characteristic diffraction peaks of ZIF-67 along with an additional broad peak originating from amorphous SiO_2 at around 2θ=20°, see **Error! Reference source not found.**. After carbonization and/or calcination, weak diffraction peaks from cobalt or cobalt oxide replaced the diffraction peaks of the ZIF-67, indicating a complete decomposition of the metal precursor. The XRD analysis also showed that Co nanoparticles were present after carbonization at 600 °C in Ar, while Co_3O_4 nanoparticles were present after calcination at 300-550 °C in air. In particular, the XRD pattern of the carbonized catalyst, Co/NC@SiO_2 (600/-), showed a weak peak from Co(111) at 2θ=44.3°, whereas the three calcined catalysts, Co_3O_4@SiO_2 (-/550), Co_3O_4@SiO_2 (600/550) and Co_3O_4@SiO_2 (600/300), showed the peak corresponding to Co_3O_4(311) at 2θ=36.8°. The catalyst prepared by direct calcination, Co_3O_4@SiO_2 (-/550), showed sharper diffraction peaks, indicating that significantly larger Co_3O_4 nanoparticles were present in this sample, see **Error! Reference source not found.**.. In general, the measured diffraction peaks were too weak to give good estimates of their nanoparticle sizes by line broadening analysis. XPS analysis did not indicate any significant changes in the chemical state of Co_3O_4, see Figure S3.

Error! Reference source not found. shows the N_2 physisorption isotherms of the investigated catalysts at 77 K. In general, the specific BET surface areas were around 802 m^2 g^{-1} for the ZIF-67@SiO_2 precursor and in the range of 626-1271 m^2 g^{-1} for the carbonized and/or calcined catalysts, see Table S1. We speculate that residual CTAB in the uncalcined SiO_2 shell limited the physisortion of N_2 in the ZIF, which could explain the relatively low surface area of the ZIF-67@SiO_2. All the carbonized and/or calcined catalysts had high total pore volumes ranging from 0.34-0.69 cm^3 g^{-1} and relatively small mesopores of around 3 nm in diameter, see DFT pore size distribution in **Error! Reference source not found.**.. The isotherm of the carbonized catalyst, Co/NC@SiO_2 (600/-), showed the highest total pore volume with a significant H4 hysteresis loop closing at around p/p^0=0.46. We believe that this hysteresis loop may originate from the restricted porosity of the N-doped carbon matrix inside the mesoporous SiO_2 shell.

Transmission electron microscopy (TEM) showed the successful formation of porous silica shells encapsulating metal nanoparticles with complete replication of the rhombic dodecahedral ZIF-67, see **Error! Reference source not found.**-9. The TEM analysis of Co_3O_4@SiO_2 (-/550) showed that the direct calcination resulted in severe sintering accompanied by the formation of large agglomerated nanoparticles of up to 75 nm in diameter, which is in good agreement with the XRD results. These particles were also visible by scanning electron microscopy (SEM) because of their large sizes, see **Error! Reference source not found.**. In contrast, the carbonization at 600°C under Ar resulted in small cobalt nanoparticles, typically <25 nm in diameter. This suggested that the carbonization of the organic linkers resulted in the formation of a N-doped carbon matrix inside the mesoporous silica shell. This carbon matrix effectively confined the size of the Co nanoparticles, see **Error! Reference source not found.**. In order to obtain active catalysts for CO oxidation, we subsequently calcined the carbonized catalysts in air at 300 °C and 550 °C, respectively. The calcination temperature appeared to have a large effect on the dispersion of Co_3O_4. While the nanoparticles in Co_3O_4@SiO_2 (600/550) were up to 65 nm in diameter, the nanoparticles in Co_3O_4@SiO_2 (600/300) were less agglomerated and typically around 20 nm in diameter, see **Error! Reference source not found.**-9. Both samples showed a significantly higher metal dispersion than Co_3O_4@SiO_2 (-/550) prepared by the direct calcination of ZIF-67@SiO_2.

In order to understand the three-dimensional distributions of Co and Co_3O_4 nanoparticles in the mesoporous nanorattle catalysts after the carbonization and the subsequent calcination, we used electron tomography in scanning TEM (STEM) to investigate Co/NC@SiO_2 (600/-) and Co_3O_4@SiO_2 (600/300). The tomography was performed by collecting tilt-series images from -68° to 68° and from -72° to 70°, respectively, using a high-angle annular dark-field (HAADF) detector. A tomographic reconstruction of Co/NC@SiO_2 (600/-) revealed that Co nanoparticles were supported on porous N-doped carbon located inside mesoporous SiO_2 shells, see **Error! Reference source not found.** and Movie S1. After calcination for 2 hours at 300 °C, the N-doped carbon was removed by combustion to leave Co_3O_4 nanoparticles on the

internal surface of the mesoporous shell in $Co_3O_4@SiO_2$ (600/300), see **Error! Reference source not found.** and Movie S2. Elemental mapping using energy dispersive X-ray (EDX) spectroscopy confirmed that the nanoparticles were confined inside the nanorattle catalyst, both before and after the calcination, see Figure 1. It is also clearly suggested that $Co/NC@SiO_2$ (600/-) had a uniform distribution of cobalt throughout the N-doped carbon, while the cobalt in $Co_3O_4@SiO_2$ (600/300) was located on the internal side of the SiO_2 shell, see **Error! Reference source not found.** b and **Error! Reference source not found.**b. The Co and O maps of $Co_3O_4@SiO_2$ (600/300) confirms that the Co nanoparticles were transformed into Co_3O_4 after the subsequent calcination. It is noted that the core in $Co/NC@SiO_2$ (600/-) is entirely filled with carbon while that in $Co_3O_4@SiO_2$ (600/300) has much less carbon, *i.e.* an empty core.

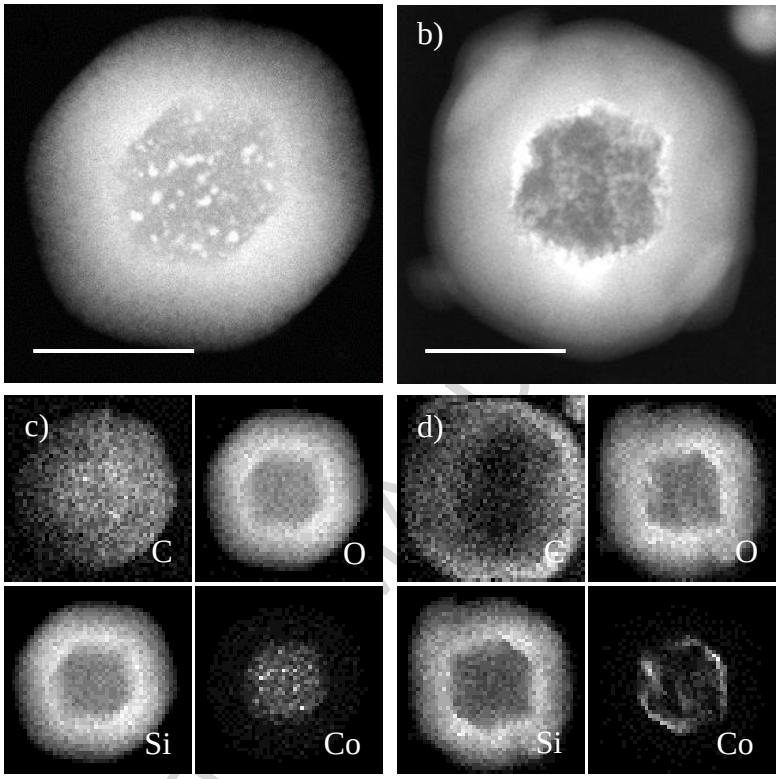

Figure 1. (a, b) Projected STEM-HAADF images of nanoparticles in $Co/NC@SiO_2$ (600/-) and $Co_3O_4@SiO_2$ (600/300), respectively. Scale bars are 100 nm. (c, d) STEM-EDS elemental maps acquired from the same particles studied by electron tomography.

In order to investigate the catalytic activity, we tested the nanorattle catalysts for CO oxidation. Figure 2 shows the so-called light-off curves of the three catalysts with the conversion of CO as a function of temperature. Because the metal loading was constant (22 wt% Co_3O_4 based on X-ray fluorescence analysis), and the same amount of catalyst were used in all experiments, the light-off curves allow direct comparison of the catalytic activity. While $Co_3O_4@SiO_2$ (-/550) and $Co_3O_4@SiO_2$ (600/550) showed similar catalytic activities to one another, reaching 50% conversion at 160 °C, $Co_3O_4@SiO_2$ (600/300) with the smallest nanoparticles showed a significantly higher activity, reaching 50% conversion at 134 °C. In agreement with previous studies,[28] these results show that decreasing the calcination temperature has a significant effect on the catalytic activity.

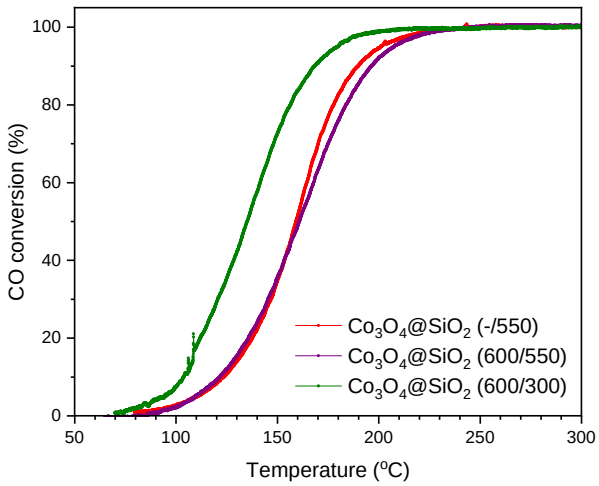

Figure 2. Conversion of CO as a function of the temperature.

As a control experiment, we tested the catalytic activity of the carbonized catalyst Co/NC@SiO_2 (600/-), see **Error! Reference source not found.**. While the initial activity was relatively poor (50% conversion at 208 °C), subsequent heating cycles resulted in a high catalytic activity (50% conversion at 134 °C). This experiment confirmed that a calcination step at around 300°C was required to oxidize Co into Co_3O_4 and activate the catalyst. For comparison, we also tested Co_3O_4/SiO_2 (-/550) prepared by simple impregnation of mesoporous silica spheres. The catalyst showed the lowest catalytic activity, reaching 50% conversion at 205°C, see Figure S14. All data from the light-off experiments are compiled in Table S2.

Co_3O_4 is known to be an active catalyst for CO oxidation at very low temperatures, but only under dry conditions (typically <1 ppm).[29–31] For instance, Jie *et al.* reported a Co_3O_4–SiO_2 nanocomposite with very high activity even at a temperature below -76°C.[32] Adsorption of H_2O however caused an unusual temperature-dependent activity curve with almost no activity at 80°C. At higher temperatures, the light-off temperatures were in the same range as reported in this work (132-160°C). The synthesis of small-sized Co_3O_4 particles with high stability and activity for CO oxidation under ambient conditions therefore remains a challenge.

3. Conclusions

In conclusion, we have reported a simple method to synthesize cobalt nanoparticles inside a mesoporous nanorattle catalyst. In this method, ZIF-67 is exploited as structural template to prepare a high surface area metal oxide shell as well as sacrificial precursor to form cobalt nanoparticles inside the shell. Furthermore, we showed that the calcination temperature had a large effect on the size and activity of the Co_3O_4 nanoparticles. By introducing a carbonization step, it was possible to decrease the final calcination temperature from 550 °C to 300 °C, which is well below the thermal decomposition temperature of ZIF-67. This resulted in a high dispersion of Co_3O_4 and, consequently, a high catalytic activity for CO oxidation. The best catalyst reached 50% conversion at 134 °C, which (under the given reaction conditions) corresponds to a site-time yield of around 22.4 mol CO/mol Co h^{-1}.

4. Experimental

Materials and Reagents: $Co(NO_3)_2{\cdot}6H_2O$ (>99.9%), 2-methylimidazole (99%), hexadecyl-trimethylammonium bromide (CTAB, ≥98%), tetraethyl orthosilicate (TEOS, 99.99% trace metals basis), methanol (HPLC Plus, ≥99.9%), absolute ethanol (≥99.8%).

The detailed synthesis and characterization of all investigated catalysts by XRD, XPS, TEM, and N_2 physisorption analysis are given in the Supporting Information.

Synthesis of metal-organic framework: ZIF-67 was synthesized from two solutions of $Co(NO_3)_2{\cdot}6H_2O$ and 2-methylimidazole in methanol. The salt solution was added to the ligand solution under vigorous stirring. The stirring was continued for 12 min and then stopped. After 24h, the purple ZIF-67 was then collected by centrifugation, washed with methanol and dried at 80 °C over night.

Synthesis of SiO_2 shell. The synthesis of ZIF-67@SiO_2 was based on a modified literature procedure.[33] In brief, TEOS was added dropwise to a stirred dispersion of ZIF-67 in ethanol, water, 2-methylimidazole and CTAB. After 24 hours, the core-shell material was collected by centrifugation, washed with ethanol and dried at 80 °C over night.

Carbonization and/or calcination. The product was carbonized in a tube furnace under flowing Ar and/or calcined in a muffle furnace in static air. In each process, the catalysts were heated for 2 hours at the desired temperature using a heating ramp of 5 °C/min.

Characterization: The prepared materials were characterized by XRD, N_2 physisorption, TGA, SEM, TEM, STEM and electron tomography. Please see supporting information for all experimental details.

Catalytic tests. The prepared catalysts were tested at atmospheric pressure in a plug flow setup equipped with a quartz fixed-bed reactor, a mass flow controller and an online non-dispersive infrared detector for quantification of CO and CO_2. The fractionated catalyst (20 mg, 180-355 µm) was diluted with quartz (100 mg, 180-355 µm) and loaded into the reactor with two pieces of quartz wool. The catalysts were fractionated to prevent external mass and heat transfer limitations and ensure high reproducibility. All catalysts were tested in a flow of 1% CO in air (50 ml/min) by decreasing the temperature from 300-30˚C by 2˚C min^{-1}.

Acknowledgements

We thank the Independent Research Fund Denmark (grant no. 5054-00119 and no. 6111-00237) for financial support. Furthermore, we acknowledge David B. Christensen for help with XPS analysis.

References

[1] L. Zhou, Z. Zhuang, H. Zhao, M. Lin, D. Zhao, L. Mai, Intricate Hollow Structures: Controlled Synthesis and Applications in Energy Storage and Conversion, Adv. Mater. 29 (2017) 1602914.
[2] X. Lai, J.E. Halpert, D. Wang, Recent advances in micro-/nano-structured hollow spheres for energy applications: From simple to complex systems, Energy Environ. Sci. 5 (2012) 5604–5618.
[3] Z. Wang, L. Zhou, X.W. Lou, Metal oxide hollow nanostructures for lithium-ion batteries, Adv. Mater. 24 (2012) 1903–1911.
[4] G. Prieto, H. Tu, N. Duyckaerts, J. Knossalla, G. Wang, F. Schüth, Hollow Nano- and Microstructures as Catalysts, Chem. Rev. 116 (2016) 14056–14119.
[5] Y. Zhang, Z. He, H. Wang, L. Qi, G. Liu, X. Zhang, Applications of hollow nanomaterials in environmental remediation and monitoring: A review, Front. Environ. Sci. Eng. 9 (2015) 770–783.
[6] J. Zhang, S.H. Chai, Z.A. Qiao, S.M. Mahurin, J. Chen, Y. Fang, S. Wan, K. Nelson, P. Zhang, S. Dai, Porous liquids: A promising class of media for gas separation, Angew. Chemie - Int. Ed. 54 (2015) 932–936.
[7] J.H. Lee, Gas sensors using hierarchical and hollow oxide nanostructures: Overview, Sensors Actuators, B Chem. 140 (2009) 319–336.
[8] N. Zhang, S. Liu, Y.-J. Xu, Recent progress on metal core@semiconductor shell nanocomposites as a promising type of photocatalyst, Nanoscale. 4 (2012) 2227–2238.
[9] S. Chen, X. Hao, X. Liang, Q. Zhang, C. Zhang, G. Zhou, S. Shen, G. Jia, J. Zhang, Inorganic nanomaterials as carriers for drug delivery, J. Biomed. Nanotechnol. 12 (2016) 1–27.
[10] J. Liu, S.Z. Qiao, J.S. Chen, X.W. (David) Lou, X. Xing, G.Q. (Max) Lu, Yolk/shell nanoparticles: new platforms for nanoreactors, drug delivery and lithium-ion batteries, Chem. Commun. 47 (2011) 12578.
[11] Q. Zhang, I. Lee, J.B. Joo, F. Zaera, Y. Yin, Core-shell nanostructured catalysts, Acc. Chem. Res. 46 (2013) 1816–1824.
[12] N. Zhang, Y. Xu, Aggregation- and Leaching-Resistant, Reusable, and Multifunctional Pd@CeO2 as a Robust Nanocatalyst Achieved by a Hollow Core−Shell Strategy, Chem. Mater. 25 (2013) 1979–1988.
[13] S. Ding, J. Song Chen, G. Qi, X. Duan, Z. Wang, E. Giannelis, L.A. Archer, X.W. Lou, Formation of SnO2 Hollow Nanospheres inside Mesoporous Silica Nanoreactors, J. Am. Chem. Soc. 50 (2011) 2–5.
[14] J. Lee, S.M. Kim, I.S. Lee, Functionalization of hollow nanoparticles for nanoreactor applications, Nano Today. 9 (2014) 631–667.
[15] Y. Zhu, J. Shi, W. Shen, X. Dong, J. Feng, M. Ruan, Y. Li, Stimuli-responsive controlled drug

release from a hollow mesoporous silica sphere/polyelectrolyte multilayer core-shell structure, Angew. Chemie - Int. Ed. 44 (2005) 5083–5087.
[16] S. Mezzavilla, C. Baldizzone, K.J.J. Mayrhofer, F. Schüth, General Method for the Synthesis of Hollow Mesoporous Carbon Spheres with Tunable Textural Properties, ACS Appl. Mater. Interfaces. 7 (2015) 12914–12922.
[17] G.-H. Wang, J. Hilgert, F.H. Richter, F. Wang, H. Bongard, B. Spliethoff, C. Weidenthaler, F. Schüth, Platinum-cobalt bimetallic nanoparticles in hollow carbon nanospheres for hydrogenolysis of 5-hydroxymethylfurfural, Nat. Mater. 13 (2014) 293–300.
[18] G.-H. Wang, K. Chen, J. Engelhardt, H. Tüysüz, H.-J. Bongard, W. Schmidt, F. Schüth, Scalable One-Pot Synthesis of Yolk − Shell Carbon Nanospheres with Yolk-Supported Pd Nanoparticles for Size-Selective Catalysis, (2018).
[19] X.W. Lou, L.A. Archer, Z. Yang, Hollow micro-/nanostructures: Synthesis and applications, Adv. Mater. 20 (2008) 3987–4019.
[20] W. Wang, M. Dahl, Y. Yin, Hollow nanocrystals through the nanoscale Kirkendall effect, Chem. Mater. 25 (2013) 1179–1189.
[21] C.C. Yec, H.C. Zeng, Synthesis of complex nanomaterials via Ostwald ripening, J. Mater. Chem. A. 2 (2014) 4843–4851.
[22] X. Fang, C. Chen, Z. Liu, P. Liu, N. Zheng, A cationic surfactant assisted selective etching strategy to hollow mesoporous silica spheres, Nanoscale. 3 (2011) 1632–1639.
[23] D. Farrusseng, A. Tuel, Perspectives on zeolite-encapsulated metal nanoparticles and their applications in catalysis, New J. Chem. (2016).
[24] H. Furukawa, K.E. Cordova, M. O'Keeffe, O.M. Yaghi, The Chemistry and Applications of Metal-Organic Frameworks, Science. 341 (2013) 1230444–1230444.
[25] J. Yang, F. Zhang, H. Lu, X. Hong, H. Jiang, Y. Wu, Y. Li, Hollow Zn/Co ZIF Particles Derived from Core-Shell ZIF-67@ZIF-8 as Selective Catalyst for the Semi-Hydrogenation of Acetylene, Angew. Chemie - Int. Ed. 54 (2015) 10889–10893.
[26] B.Y. Xia, Y. Yan, N. Li, H. Bin Wu, X.W. Lou, X. Wang, A metal–organic framework-derived bifunctional oxygen electrocatalyst, Nat. Energy. 1 (2016) 15006.
[27] X. Cao, C. Tan, M. Sindoro, H. Zhang, Hybrid micro-/nano-structures derived from metal–organic frameworks: preparation and applications in energy storage and conversion, Chem. Soc. Rev. 46 (2017) 2660–2677.
[28] J. Zheng, W. Chu, H. Zhang, C. Jiang, X. Dai, CO oxidation over Co3O4/SiO2 catalysts: Effects of porous structure of silica and catalyst calcination temperature, J. Nat. Gas Chem. 19 (2010) 583–588.
[29] D.A.H. Cunningham, T. Kobayashi, N. Kamijo, M. Haruta, Influence of dry operating conditions: observation of oscillations and low temperature CO oxidation over Co3O4 and Au/Co3O4 catalysts, Catal. Letters. 25 (1994) 257–264.
[30] M. Skoglundh, E. Fridell, B. Andersson, P. Thorm, Low-Temperature CO Oxidation over Platinum and Cobalt Oxide Catalysts, J. Catal. 310 (1999) 300–310.
[31] X. Xie, Y. Li, Z.Q. Liu, M. Haruta, W. Shen, Low-temperature oxidation of CO catalysed by Co3O4 nanorods, Nature. 458 (2009) 746–749.
[32] C.J. Jia, M. Schwickardi, C. Weidenthaler, W. Schmidt, S. Korhonen, B.M. Weckhuysen, F. Schüth, Co3O4-SiO2 Nanocomposite: A very active catalyst for CO oxidation with unusual catalytic behavior, J. Am. Chem. Soc. 133 (2011) 11279–11288.
[33] G. Zhan, H.C. Zeng, ZIF-67-Derived Nanoreactors for Controlling Product Selectivity in CO2 Hydrogenation, ACS Catal. 7 (2017) 7509–7519.

Highlights

- Zeolitic imidazolate frameworks are promising starting points for synthesis of advanced nanorattle catalysts
- ZIF-67 can serve as both structural template and sacrificial cobalt precursor
- Heat treatments control the three-dimensional distribution of Co_3O_4 nanoparticles
- The dispersion of Co_3O_4 has a large effect on the catalytic activity for CO oxidation